INTERNATIONAL JOURNAL OF OPTIMIZATION IN CIVIL ENGINEERING
Int. J. Optim. Civil Eng., 2018; 8(3):453-467

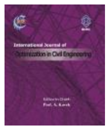

ANN BASED MODELING FOR HIGH STRENGTH CONCRETE BEAMS WITH SURFACE MOUNTED FRP LAMINATES

K. Suguna*, †, P.N. Raghunath, J. Karthick and R. Uma Maheswari
Department of Civil and Structural Engineering, Annamalai University, India

ABSTRACT

This study focuses on using an artificial neural network (ANN) based model for predicting the performance of high strength concrete (HSC) beams strengthened with surface mounted FRP laminates. Eight input parameters such as geometrical properties of the beam and mechanical properties of FRP laminates were considered for this study. Back propagation network with Lavenberg-Marquardt algorithm has been chosen for the proposed network, which has been implemented using the programming package MATLAB. In the present study, comparison has been made between the experimental results and those predicted through neural network modeling. The amount of MAPE and RMSE were predicted and were found to be acceptable range. The statistical indicators such as correlation co-efficient (r) and co-efficient of determination (R^2) were also predicted to estimate the accuracy of results obtained through ANN modeling. The results predicted through ANN modeling exhibit good correlation with the experimental results.

Keywords: ANN; FRP; beams; high strength concrete; static.

Received: 20 September 2017; Accepted: 12 November 2017

1. INTRODUCTION

Now-a-days, strengthening of high strength concrete members with surface mounted fibre reinforced polymer laminates (FRP) has proved to be an effective and appropriate technique to improve their performance under service loads or ultimate loads [1]. This technique has several advantages because of the inherent characeteristics of FRP material such as high strength-to-weight ratio, low maintenance cost and higher corrosion resistance [2]. Fibre-reinforced polymer (FRP) is a composite material made of a polymer matrix reinforced with fibres. FRP composites are becoming an alternative material for rehabilitation and retrofitting projects around the world [3]. Depending on the design objectives, these

*Corresponding author: Department of Civil and Structural Engineering, Annamalai University, India
sugunaraghunath@gmail.com (K. Suguna)

materials can be used to improve one or more of the structural member characteristics such as load capacity, ductility and durability [4,5]. Design of structural strengthening applications using surface mounted FRP composites is usually based on conventional design approaches with improvements to account for the presence and characteristics of the FRP material. In the meantime, soft computing and artificial intelligence techniques like artificial neural networks (ANN), adaptive neuro-fuzzy inference system (ANFIS) and optimization algorithms (GA) have also been used in various civil engineering applications. An effort has been taken by some researchers in the area of soft computing and artificial intelligence techniques [5-8]. Shanmugavelu et al [5] proposed an ANN based model for predicting the performance characteristics of reinforced concrete beams strengthened with glass fibre reinforced polymer laminates. The model was developed using general regression neural network (GRNN) to predict different target parameters such as yield load, deflection at yield load, ultimate load, deflection at ultimate load and ductility ratio respectively. The authors reported that the proposed artificial neural network based model performed well to predict the target parameters. Metwally [6] predicted the flexural capacity of reinforced concrete beams using artificial neural network. The feed-forward back-propagation neural network was applied to predict the flexural load capacity. The author reported that the proposed ANN model provides accurate results in calculating the ultimate flexural load. Amani and Moeini [7] predicted the shear strength of reinforced concrete (RC) beams using ANN and ANFIS based model. Back-Propagation (BP) algorithm was used to predict the shear strength of RC beams. The authors reported that the ANN based model was better than that of ANFIS based model and the two models provide better prediction when compared to ACI and ICI empirical codes. Pannirselvam et al [8] developed an ANN based model for predicting the effectiveness of glass fibre reinforced polymer laminates on the performance of RC beams. The results of fifteen reinforced concrete beams with an ANN based model were reported in this study. The authors reported that the ANN based model provided a reasonable prediction of the target parameters. The predicted results are in good agreement with the experimental results. This study has been taken up for predicting the performance of high strength concrete (HSC) beams strengthened with surface mounted FRP laminates using an artificial neural network (ANN) based model.

2. MATERIALS AND METHODS

2.1 Artificial neural network (ANN)

An Artificial Neural Network (ANN) is an information processing paradigm that is inspired by the way biological nervous systems such as brain and process information. The key element of this paradigm is the novel structure of the information processing system. It is composed of a large number of highly interconnected processing elements (neurons) working in unison to solve specific problems. There are other ANNs which are adaptive systems used to model things such as environments and population. The ANN attempts to recreate the computational mirror of the biological neural network, although it is not comparable since the number and complexity of neutrons used in a biological neural network is many times more than those in an artificial neutral network. An ANN is comprised of a network of artificial neurons (also known as "nodes"). These nodes are connected to each other and the strength of their connection to one another is assigned a value based on their strength: inhibition (maximum being -1.0) or excitation (maximum being +1.0). If the value of the connection is high, then it indicates that there is a strong connection. Within each node's design, a transfer function is built in. There are three types of neutrons in an ANN, input nodes, hidden nodes, and output nodes. The neural network architecture is shown in Fig. 1.

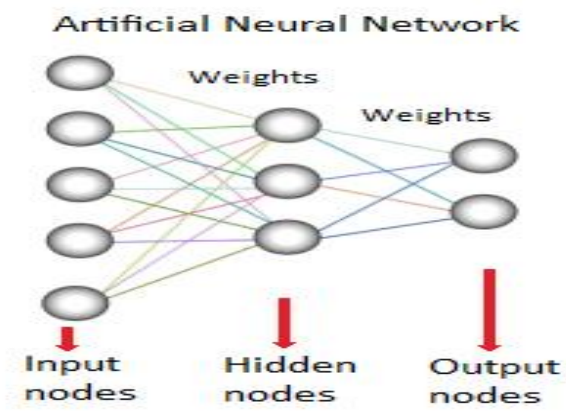

Figure 1. Architecture of Neural Network

2.2 Human nervous system versus artificial neural network

Artificial neuron is a basic building block of every artificial neural network. Its design and functionalities are derived from observation of a biological neuron that is basic building block of biological neural networks (systems) which includes the brain, spinal cord and peripheral ganglia. Similarities in design and functionalities can be seen in Fig. 2. Fig. 2(a) represents a biological neuron with its soma, dendrites and axon and Fig. 2(b) represents an artificial neuron with its inputs, weights, transfer function, bias and outputs.

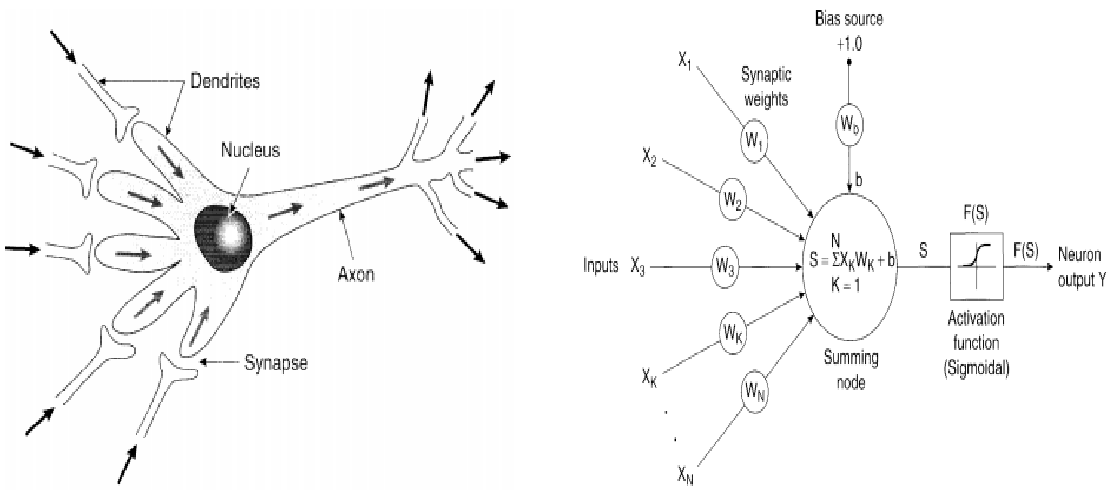

(a) Biological neural network (b) Artificial neural network

Figure 2. Structure of Biological Neural Network and Artificial Neural Network

In case of biological neuron, information comes into the neuron via dendrite; soma processes the information and passes it on via axon. In case of artificial neuron, information comes into the body of an artificial neuron via inputs that are weighted (each input can be individually multiplied with a weight). The body of an artificial neuron then sums the weighted inputs, bias and "processes" the sum with a transfer function. At the end, an artificial neuron passes the processed information via output(s).

2.3 Data used in ANN modeling

The geometrical properties of the beam such as length (L), breadth (B) and depth (D) of the section, reinforcement ratio (ρ), characteristic compressive strength of concrete (f_{ck}) and the mechanical properties of FRP laminates such as tensile strength (f_{frp}) and elasticity modulus (E_{frp}) were considered as the input parameters. The experimental results of all the test beams such as yield load (P_y), deflection at yield load (Δ_y), service load (P_s), deflection at service load (Δ_s), ultimate load (P_u), deflection at ultimate load (Δ_u) and deflection ductility (DD) were considered as the target parameters. The input and target parameters for ANN modeling are presented through Tables 1 and 2.

Table 1: Input parameters for ANN modeling

Beam designation	L (mm)	B (mm)	D (mm)	T (mm)	f_{frp} (MPa)	E_{frp} (GPa)	ρ_s (%)	f_{ck} (MPa)
RA	3000	150	250	0.00	0.0	0.00	0.419	64.0
RAC3	3000	150	250	3.00	126.2	7.47	0.419	64.0
RAC5	3000	150	250	5.00	156.0	11.39	0.419	64.0
RAU3	3000	150	250	3.00	446.9	13.97	0.419	64.0
RAU5	3000	150	250	5.00	451.5	17.37	0.419	64.0
RB	3000	150	250	0.00	0.00	0.00	0.628	64.0
RBC3	3000	150	250	3.00	126.2	7.47	0.628	64.0
RBC5	3000	150	250	5.00	156.0	11.39	0.628	64.0
RBU3	3000	150	250	3.00	446.9	13.97	0.628	64.0
RBU5	3000	150	250	5.00	451.5	17.37	0.628	64.0

Table 2: Target parameters for ANN modeling

Beam designation	P_y (kN)	Δ_y (mm)	P_s (kN)	Δ_s (mm)	P_u (kN)	Δ_u (mm)	DD
RA	29.42	7.91	27.79	14.03	41.68	21.05	2.66
RAC3	36.77	9.02	34.32	22.31	51.48	33.46	3.70
RAC5	46.58	10.10	44.13	31.21	66.19	46.81	4.63
RAU3	51.48	11.42	47.39	35.50	71.09	53.26	4.66
RAU5	53.70	10.74	52.30	38.14	78.45	57.21	5.32
RB	39.22	8.11	35.95	20.85	53.93	31.28	3.86
RBC3	51.48	11.35	40.86	24.15	61.29	36.23	3.19
RBC5	53.24	12.41	42.49	37.94	63.74	56.91	4.59
RBU3	58.80	12.85	58.83	40.69	88.25	61.04	4.75
RBU5	63.00	12.69	67.00	43.73	100.51	65.59	2.66

2.4 Steps involved in ANN modeling

In this stage, the input data are divided into three groups which are train data, validate data and test data. The step-wise procedure for ANN modeling is presented through Figs. 3 to 10.

2.4.1 Building the network

This stage, specifies the number of hidden layers, neurons in each layer, transfer function in each layer, training function, weight/bias learning function and performance function as shown in Figs. 3 and 4.

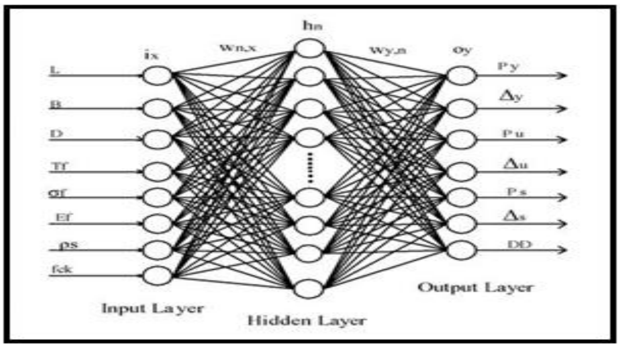

Figure 3. Architecture of proposed NN model

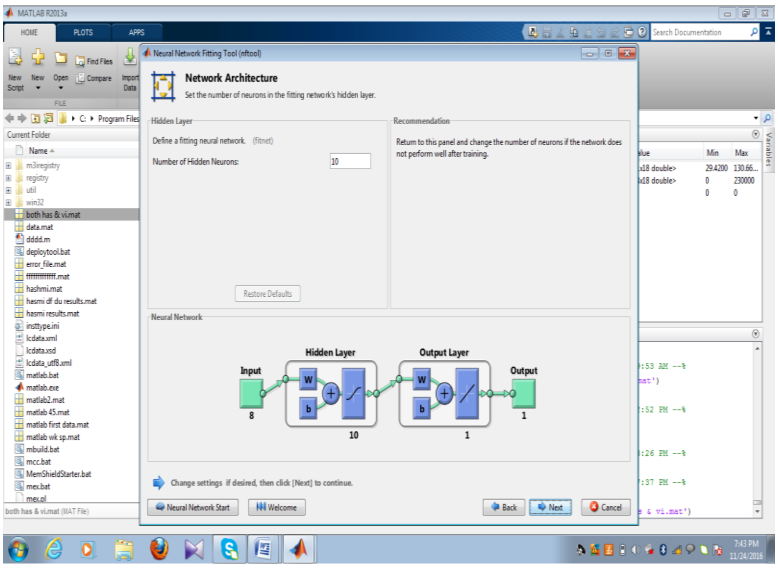

Figure 4. Neural network architecture

2.4.2 Training the network

Back propagation algorithms are used to developing the artificial neural network. The training processes are shown through Figs. 5 and 6. The weights are adjusted to make the actual outputs (predicted) close to the target (measured) outputs of the network.

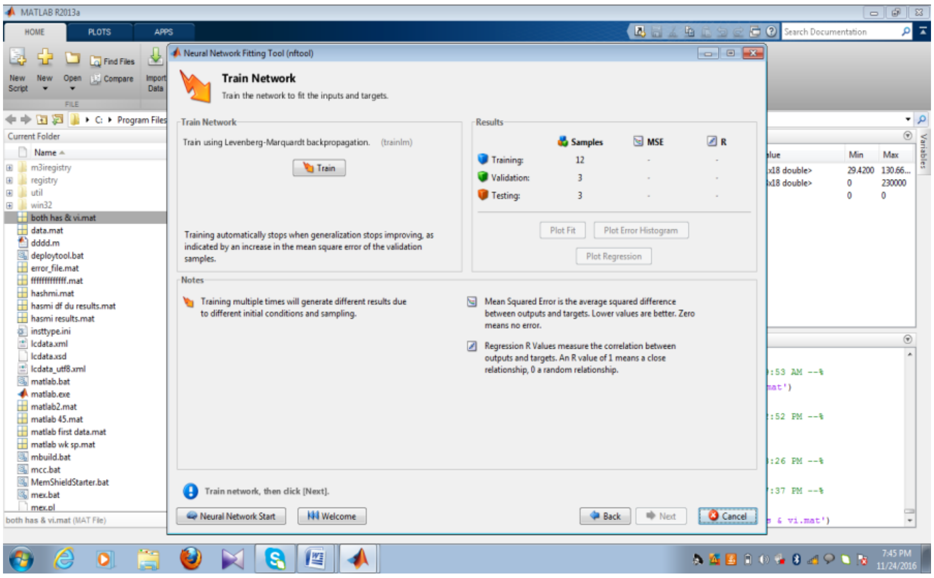

Figure 5. Training Network Wizards

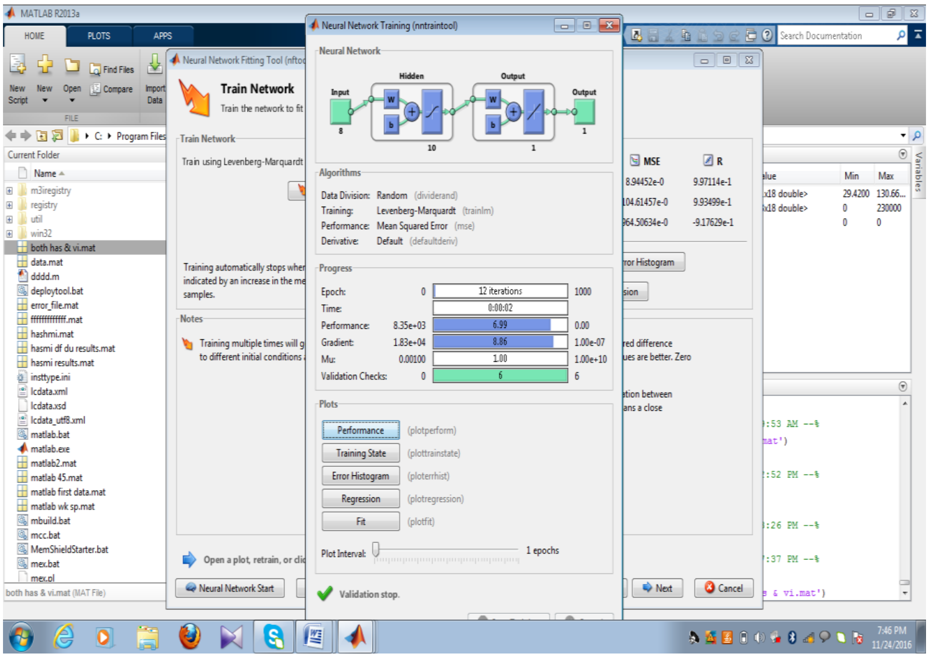

Figure 6. Neural Network Training

2.4.3 Test performance of model

The fitness of the developed model is shown through Figs. 7 to 10. At this stage, unseen data are exposed to the model.

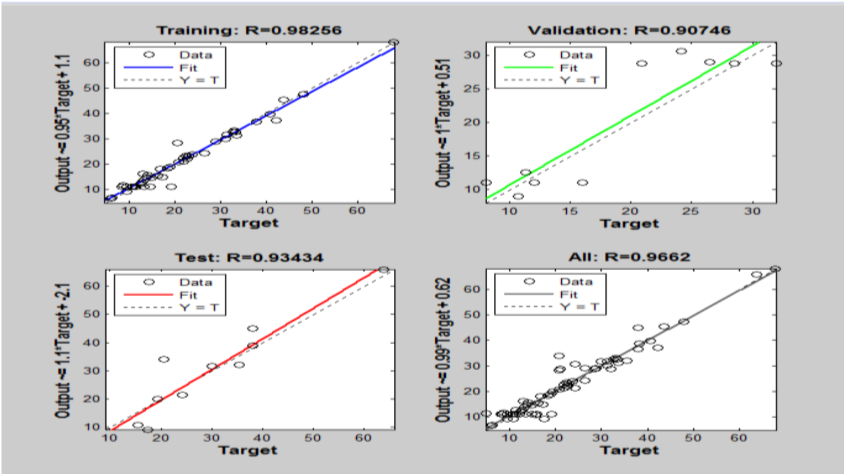

Figure 7. Neural Network Regression Plot

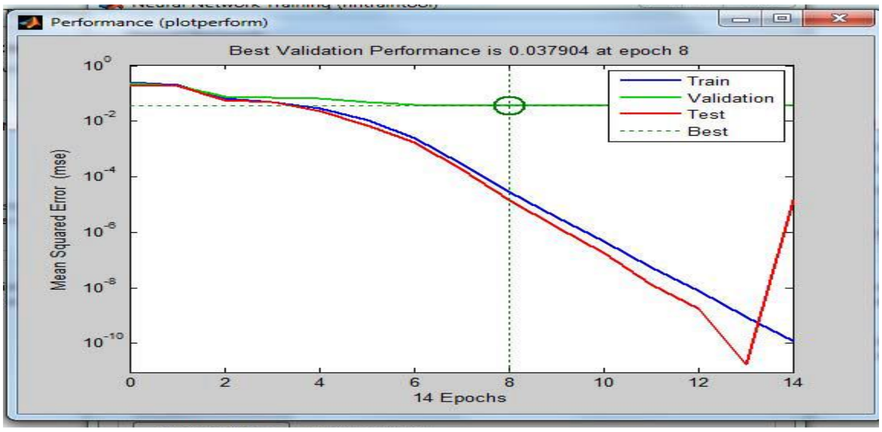

Figure 8. Neural Network Training Performance Plot

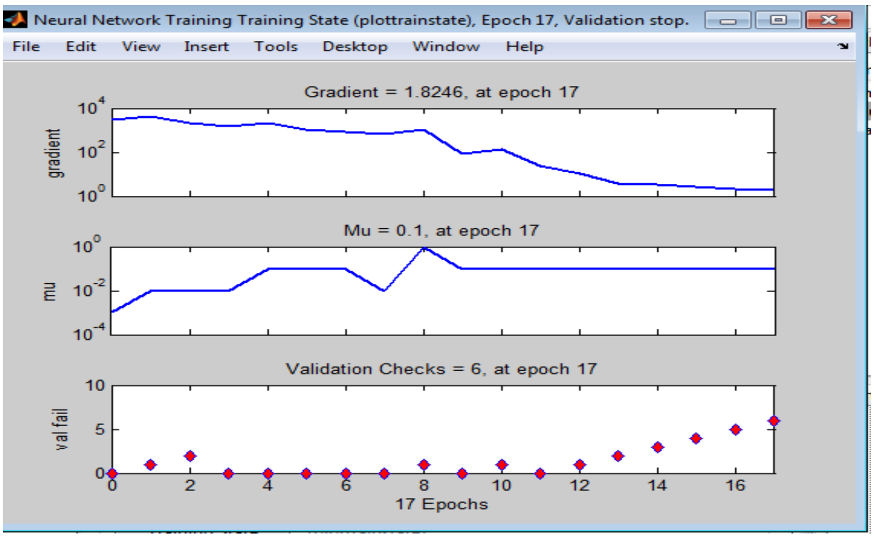

Figure 9. Neural Network Training State

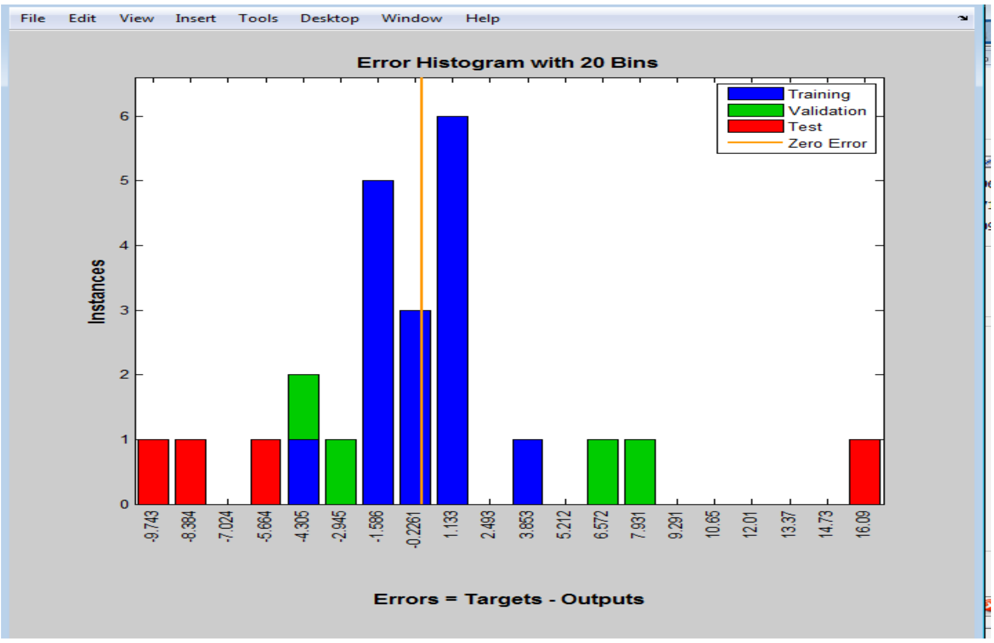

Figure 10. Neural Network Error Histogram State

2.5 Data used for validating the ANN results

The experimental results pertinent to this problem from other researchers published work were used for the purpose of validating the ANN model. Data such as length of the section (L), breath of the section (B), depth of the section (D), thickness of FRP laminates (t_{frp}), tensile strength of FRP laminates (f_{frp}), elasticity modulus of FRP laminates (E_{frp}), reinforcement ratio (ρ) and characteristic strength of concrete at 28 days (f_{ck}) taken from the research works **[]** are presented through Tables 3 to 4.

Table 3: Input parameters for ANN modeling

Authors name	Beam designation	L (mm)	B (mm)	D (mm)	T (mm)	f_{frp} (MPa)	E_{frp} (GPa)	ρ_s (%)	f_{ck} (MPa)
Hashemi et al. (2009)	AH0	3000	150	250	0.00	0.0	0.00	0.107	77.0
	AH1	3000	150	250	0.05	3850.0	230.00	0.107	77.0
	AH4	3000	150	250	0.18	3850.0	230.00	0.107	77.0
	ACG3	3000	150	250	0.48	3850.0	230.00	0.107	77.0
	BHO	3000	150	250	0.00	0.0	0.00	0.203	77.0
	BH1	3000	150	250	0.05	3850.0	230.00	0.203	77.0
	BH4	3000	150	250	0.18	3850.0	230.00	0.203	77.0
	BCG3	3000	150	250	0.48	3850.0	230.00	0.203	77.0
Phalguni Mukhopadhyaya et al. (1998)	SAB1	3000	150	250	0.00	0.0	0.00	0.565	66.7
	FS1	3000	150	250	2.50	786.5	152.70	0.565	53.3
	FS2	3000	150	250	3.50	786.5	229.00	0.565	54.0
	FS3	3000	150	250	3.50	786.5	229.00	0.565	66.5
	FS4	3000	150	250	3.50	786.5	229.00	0.565	79.7
	FS5	3000	150	250	3.50	786.5	229.00	0.565	66.6

Rabinovith et al. (2003)	A1	2500	200	200	0.00	0.0	0.00	0.482	76.3
	A2	2500	200	200	1.20	2800.0	165.00	0.482	76.3
	A3	2500	200	200	1.20	2800.0	165.00	0.482	76.3
	B1	2500	200	200	0.00	0.0	0.00	0.482	76.3
	B2	2500	200	200	1.20	2800.0	165.00	0.482	76.3
Grace et al. (2002)	C	2744	152	254	0.00	0.0	0.00	0.521	65.2
	C-1	2744	152	254	0.13	2413.0	231.00	0.521	65.2
	C-2	2744	152	254	1.30	2413.0	231.00	0.521	65.2
	C-3	2744	152	254	1.90	2413.0	231.00	0.521	65.2
	H-50-2	2744	152	254	1.00	1324.0	379.00	0.521	65.2
	H-75-2	2744	152	254	1.50	1324.0	379.00	0.521	65.2
Mahfuz ud darain et al. (2016)	CB	3300	125	250	0.00	0.0	0.00	0.724	60.5
	CBC8P1	3300	125	250	0.17	4900.0	230.00	0.724	60.5
	CBC8P2	3300	125	250	0.34	4900.0	230.00	0.724	60.5
	CBC10P1	3300	125	250	0.17	4900.0	230.00	0.724	60.5
	CBC10P2	3300	125	250	0.34	4900.0	230.00	0.724	60.5
	CBC10PA	3300	125	250	0.34	4900.0	230.00	0.724	60.5
Maghsoudi et al. (2009)	AH0	3000	150	250	0.00	0.0	0.00	1.200	77.0
	AHF	3000	150	250	0.94	2800.0	165.00	1.200	77.0
	AHD	3000	150	250	0.67	2800.0	165.00	1.200	77.0
	BH0	3000	150	250	0.00	0.0	0.00	2.400	77.0
	BHF	3000	150	250	0.94	2800.0	165.00	2.400	77.0
	BHD	3000	150	250	0.67	2800.0	165.00	2.400	77.0
Fanning et al. (2001)	F1	3000	155	240	0.00	0.0	0.00	0.912	80.0
	F2	3000	155	240	0.00	0.0	0.00	0.912	80.0
	F3	3000	155	240	1.20	2400.0	155.00	0.912	80.0
	F4	3000	155	240	1.20	2400.0	155.00	0.912	80.0
	F5	3000	155	240	1.20	2400.0	155.00	0.912	80.0
	F6	3000	155	240	1.20	2400.0	155.00	0.912	80.0
	F7	3000	155	240	1.20	2400.0	155.00	0.912	80.0
	F8	3000	155	240	1.20	2400.0	155.00	0.912	80.0
Gopinathan et al. (2016)	CBHSC	3000	150	250	0.00	0.0	0.00	0.603	67.0
	C3HSC	3000	150	250	3.00	126.2	7.47	0.603	67.0
	C5HSC	3000	150	250	5.00	156.0	11.39	0.603	67.0
	W3HSC	3000	150	250	3.00	147.4	6.86	0.603	67.0
	W5HSC	3000	150	250	5.00	178.1	8.99	0.603	67.0
	U3HSC	3000	150	250	3.00	446.9	13.97	0.603	67.0

Table 4: Source Data used for Validation of Predicted Results

Author	Test Beam	Yield Load (kN)	Deflection at Yield Load (mm)	Service Load (kN)	Deflection at Service Load (mm)	Ultimate Load (kN)	Deflection at Ultimate Load (mm)	Deflection Ductility
Hashemi et al.(2009)	AH0	63.93	21.00	54.17	68.00	81.25	102.00	4.35
	AH1	69.50	13.00	59.93	33.61	89.90	50.42	3.88
	AH4	64.70	9.83	78.20	21.90	117.30	32.85	3.34
	ACG3	67.33	10.37	69.33	17.47	104.66	26.20	2.53
	BH0	122.22	13.33	99.68	63.80	149.52	95.70	7.18
	BH1	130.00	14.11	100.00	42.16	150.00	63.24	4.48
	BH4	118.00	12.86	111.33	20.61	167.00	30.92	2.40
	BCG3	130.66	13.80	108.22	17.33	162.33	26.00	1.88
Phalguni et al. (1998)	SAB1	170.50	22.17	133.26	19.07	199.90	28.60	1.29
	FS1	190.25	25.92	140.93	18.32	211.40	27.48	1.06
	FS2	179.00	30.60	131.27	20.61	196.90	30.91	1.10
	FS3	199.90	27.14	146.53	22.61	219.80	33.92	1.52
	FS4	215.35	20.63	155.53	26.40	233.30	39.60	2.16
	FS5	214.70	19.24	154.6	24.2	231.90	36.36	1.58
Rabinovith et al. (2003)	A1	65.00	9.90	50.28	33.33	75.42	50.00	5.05
	A2	140.00	10.50	104.40	11.33	156.60	17.00	1.62
	A3	135.00	11.00	118.67	12.67	178.00	19.00	1.72
	B1	109.00	12.00	73.33	32.67	110.00	49.00	4.04
	B2	155.00	11.50	124.93	12.67	187.40	19.00	1.65
Grace et al.(2002)	C	82.30	14.00	63.80	33.00	95.70	49.52	3.55
	C-1	85.90	13.20	67.93	18.93	101.90	28.40	2.15
	C-2	132.60	16.00	88.40	10.67	132.60	16.00	1.00
	C-3	107.70	13.50	89.60	14.73	134.40	22.10	1.64
	H-50-2	97.90	15.20	76.53	23.73	114.80	35.60	2.33
	H-75-2	113.90	13.70	87.20	19.47	130.80	29.20	2.13
Mahfuz ud darain et al. (2016)	CB	36.00	15.00	26.00	22.87	39.00	34.30	2.29
	C8P1	50.00	14.90	47.33	26.47	71.00	39.70	2.66
	C8P2	55.00	15.20	51.33	20.87	77.00	31.30	2.06
	C10P1	54.00	16.60	54.67	28.87	82.00	43.30	2.60
	C10P2	69.00	23.70	58.00	28.47	87.00	42.70	1.80
	C10P2A	80.00	24.70	70.00	31.93	105.00	47.90	1.90
Fanning et al.(2001)	F1	53.00	12.18	45.53	31.33	68.30	47.00	3.86
	F2	53.50	12.12	45.27	30.00	67.90	45.00	3.71
	F3	82.90	11.95	73.93	14.67	110.90	22.00	1.84
	F4	83.60	12.50	79.00	16.00	118.50	24.00	1.92
	F5	85.60	10.96	66.67	11.33	100.00	17.00	1.55
	F6	85.60	12.73	68.67	13.33	103.00	20.00	1.57
	F7	83.70	12.50	65.00	12.00	97.50	18.00	1.44
	F8	78.30	13.10	54.67	10.67	82.00	16.00	1.22
Maghsou di et al. (2009)	AH0	63.73	11.89	54.17	48.00	81.25	72.00	6.05
	AHF	76.70	11.13	68.67	15.49	103.00	23.23	2.08

	AHD	71.30	10.15	67.33	13.31	101.00	19.96	1.97
	BHF	122.00	13.04	89.93	38.00	134.90	57.00	4.28
	BHD	124.00	12.18	107.33	16.25	161.00	24.38	1.87
	CBHSC	35.00	2.34	108.76	16.70	163.30	25.05	2.07
Gopinathan et al. (2016)	C3HSC	40.00	3.09	36.67	4.69	55.00	7.03	3
	C5HSC	45.00	3.78	43.33	5.97	65.00	8.95	2.89
	W3HSC	45.00	3.91	60.00	8.00	90.00	12.00	3.17
	W5HSC	50.00	4.17	46.67	6.29	70.00	9.44	2.414
	U3HSC	68.00	4.32	66.67	8.55	100.00	12.82	3.07
	U5HSC	76.00	4.46	80.00	10.75	120.00	16.13	3.73

3.0 RESULTS AND DISCUSSION

The proposed Artificial Neural Network (ANN) based model was performed well for predicting the performance parameters of FRP strengthened high strength concrete beams such as yield load, deflection at yield load, service load, deflection at service load, ultimate load, deflection at ultimate load, and deflection ductility. To ascertain the accuracy of the models, scatter plots were drawn between the experimental results and those results predicted through ANN model as shown in Fig. 11.

The predicted versus experimental value for the yield load and deflection at yield load are shown through Figs. 11(a) and (b).The ANN predictions for the yield load resulted in a MAPE of 5.23%, a RMSE of 6.375, a correlation co-efficient of 0.934 and a co-efficient of determination of 0.981 was observed at 50 epochs. For the deflection at yield load, the ANN resulted in a correlation co-efficient of 0.926, a co-efficient of determination of 0.966, a RMSE of 1.055 and a MAPE of 5.31% was observed at 30epochs.

The predicted versus experimental value for the service load and deflection at service load are presented through Figs. 11(c) and (d). For the service load, the ANN yields a correlation co-efficient of 0.918, co-efficient of determination of 0.968, a RMSE of 6.621and a MAPE of 5.99% was observed at 37 epochs. The ANN predictions for the deflection at service load resulted in a correlation co-efficient of 0.927, a co-efficient of determination of 0.980, a RMSE of 1.786 and a MAPE of 6.07% was observed at 17epochs.

The ANN prediction for the ultimate load resulted in a correlation co-efficient of 0.953, a co-efficient of determination of 0.960, a RMSE of 9.542 and a MAPE of 5.85% was observed at 60 epochs. The ANN resulted in a correlation co-efficient of 0.937, a co-efficient of determination of 0.974, a RMSE of 3.121 and a MAPE of 6.93% was observed at 40epochs in the prediction of deflection at ultimate load. Good convergence was observed between the experimental results and predicted results for ultimate load and deflection at ultimate load as shown through Figs. 11 (e) and (f).

The predicted versus experimental value for the deflection ductility is shown in Fig. 11 (g). The ANN resulted in a correlation co-efficient of 0.966, a co-efficient of determination of 0.988, a RMSE of 6.352 and a MAPE of 9.54% was observed at 18epochs in the prediction of deflection ductility. Good convergence was observed between the experimental results and the predicted results. The summary of performance evaluation of ANN model is reported in Table 5.

The results of ANN model have been validated using other researcher's results to improve its accuracy. The input and target parameters considered for the validation of results are presented in Tables 3 and 4. The results predicted through ANN modeling are presented through Fig. 11 (a) to (g) in the form of scatter plots. From Fig. 11 (a) to (g), it can be observed that most of the points fall along the diagonal line for the ANN prediction model. It shows that the results predicted through ANN model are in very good agreement with the experimental results.

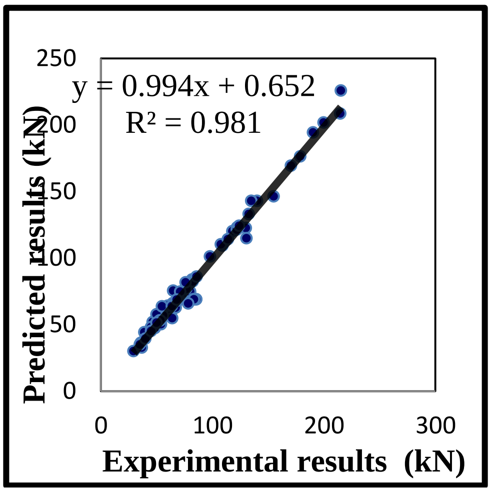

(a) Yield load

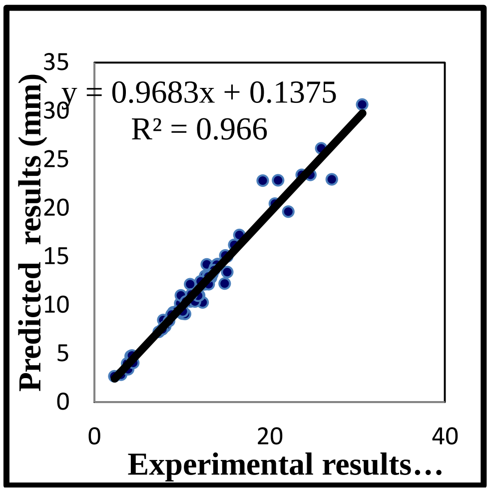

(b) Deflection at Yield Load

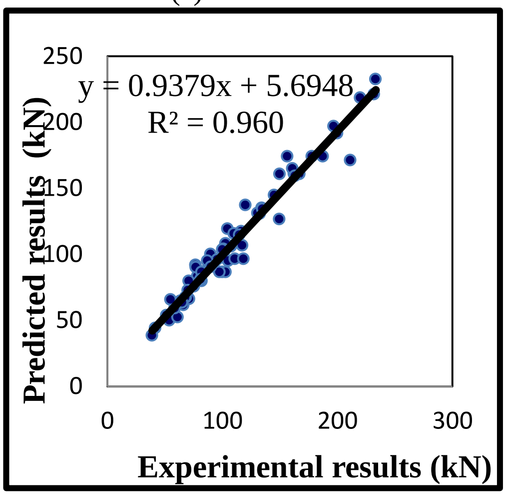

(c) Service Load

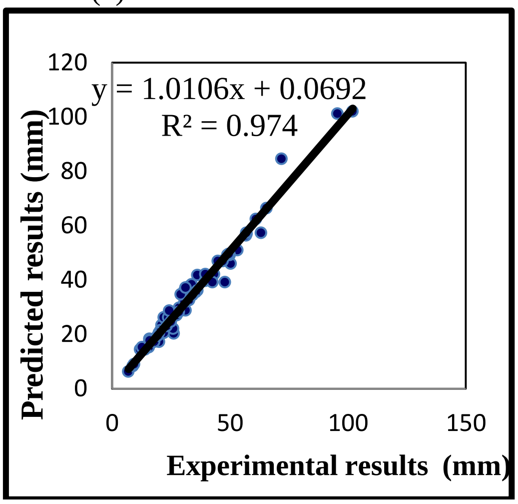

(d) Deflection at Service Load

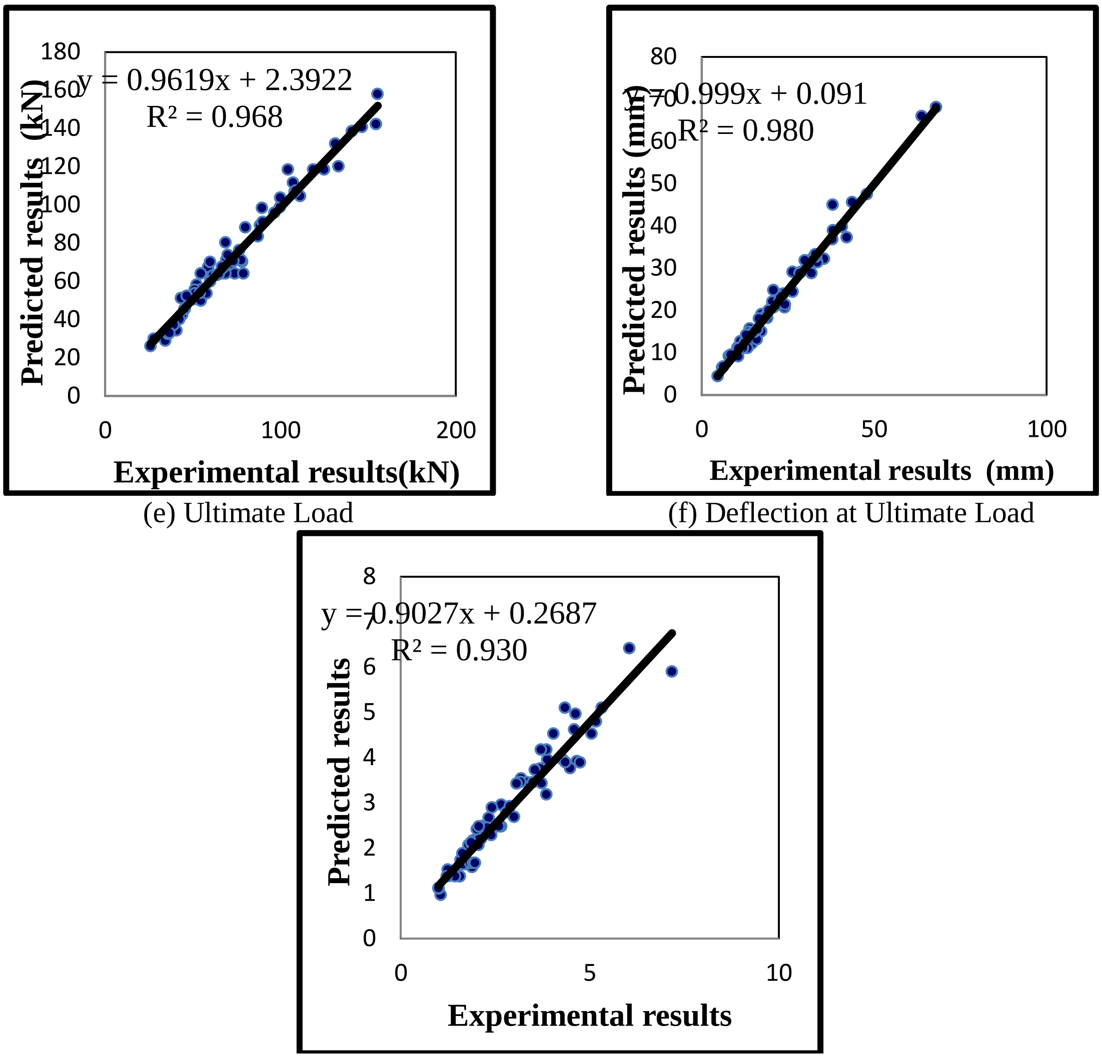

(e) Ultimate Load (f) Deflection at Ultimate Load

(g) Deflection Ductility

Figure 11. Comparison of Experimental and Predicted Results

Table 5: Performance evaluation of ANN model

S.NO	Output parameters	r	RMSE	MAPE	R^2
1	Yield load (kN)	0.934	6.375	5.230	0.981
2	Deflection at Yield load (mm)	0.925	1.055	5.310	0.966
3	Ultimate load(kN)	0.954	9.542	5.850	0.960
4	Deflection at ultimate load(mm)	0.938	3.121	6.930	0.974
5	Service load(kN)	0.918	6.624	5.990	0.968
6	Deflection at service load (mm)	0.927	1.786	6.070	0.980
7	Deflection ductility	0.966	0.351	9.540	0.938

4. CONCLUSIONS

This main aim of this study focuses on using an artificial neural network (ANN) based model for predicting the performance of high strength reinforced concrete (HSC) beams strengthened with surface mounted FRP laminates. The performances of the models were evaluated and the results predicted through ANN modeling were compared with the experimental results. The results predicted through ANN modeling exhibited better convergence with the experimental results. Also the results show that ANN modeling is a more accurate and reliable tool for evaluating the performance of high strength concrete beams strengthened with FRP laminates under static loading condition. This is evident from the values of correlation co-efficient (r), RMSE, MAPE and R^2, which are global, more realistic and meaningful error types. It can be seen from the obtained results that the lowest RMSE and MAPE and the highest r and R^2. A correlation co-efficient of 0.918 to 0.966 and a co-efficient of determination of 0.938 to 0.981 was observed for HSC beams strengthened with FRP laminates while predicting the convergence through scatter plots.

REFERENCES

1. Gopinathan TK, Raghunath PN, Suguna K. Static and cyclic performance of HSC beams with GFRP laminates, *Asian J Eng Technol* 2016; **4**: 2321-2462.
2. Gopinathan TK, Raghunath PN, Suguna K. Regression model for static and cyclic performance of HSC beams with GFRP laminates, *Indian J Sci Technol* 2016; **9**: 974-80.
3. Parthiban B, Suguna K, Raghunath PN. Hybrid fibre reinforced concrete beams strengthened with externally bonded GFRP laminates, *Asian J Eng Technol* 2014; **2**: 2319-39.
4. Rajeshguna R, Suguna K, Raghunath PN. Steel fibre reinforced concrete beams with externally bonded FRP laminates, *Asian J Eng Technol* 2014; **2** 2321-24.
5. Shanmugavelu VA, Ramachandran N, Raghunath PN, Suguna K. Experimental and analytical studies on reinforced concrete beams with GFRP laminates, *Int J Appl Eng Res* 2016; **1**: 1950-53.
6. Ibrahim M. Intelligent predicting system for modelling of reinforced concrete of flexurally strengthened beams with CFRP laminates, *Build Res J* 2014; **61**: 25-42.
7. Amani J, Moeini R. Prediction of shear strength of reinforced concrete beams using adaptive neuro-fuzzy inference system and artificial neural network, *Sci Iran Trans A;Civil Eng* 2012; **19**: 242-48.
8. Pannirselvam N, Nagaradjane V, Chandramoul, Ravindrakrishna M. Artificial neural network model for performance evaluation of RC rectangular beams with externally bonded glass fibre reinforced polymer reinforcement, *ARPN J Eng Appl Sci* 2010; **5**: 77-85.
9. Hashemi SH, Rahgozar R, Maghsoudi AA. Flexural testing of high strength reinforced concrete beams strengthened with CFRP sheets, *IJE Transact B: Applicat* 2009; **22**: 131-40.
10. Phalguni M, Narayan Swamy, and Cyril L. Optimizing structural response of beams strengthened with GFRP plates, *J Compos Construct* 1998; **2**: 87-95.
11. Rabinovitch O, Frostig Y. Experiments and analytical comparison of RC beams strengthened with CFRP composites, *J Compos: part B* 2003; **34**: 663-77.
12. Grace F, George AS, Ragheb F. An innovative ductile composite fabric for strengthening concrete structures, *ACI Struct J* 2002; **99**: 692-700.

13. Mahfouz Ud Darain, Mohd Zamin Jumaat, Ahmad Azim Shurkri, Obaydullah M, Nazmul Huda, Akterhosen, Nursat Hoque. Strengthening of RC beams using externally bonded reinforcement combined with near surface mounted technique, *Polym* 2016; **8**: 261-67.
14. Paul Fanning Oliverkelly. Ultimate response of rc beams strengthened with cfrp plates, *J Compos Construct* 2001; **5**: 122-27.